

cGMP Binding to Noncatalytic Sites on Mammalian Rod Photoreceptor Phosphodiesterase Is Regulated by Binding of Its γ and δ Subunits*

(Received for publication, September 28, 1998, and in revised form, April 5, 1999)

Hongmei Mou‡, Hector J. Grazio III‡, Terry A. Cook§, Joseph A. Beavo§, and Rick H. Cote‡¶

From the ‡Department of Biochemistry and Molecular Biology, University of New Hampshire, Durham, New Hampshire 03824 and the §Department of Pharmacology, University of Washington, Seattle, Washington 98195

The binding of cGMP to the noncatalytic sites on two isoforms of the phosphodiesterase (PDE) from mammalian rod outer segments has been characterized to evaluate their role in regulating PDE during phototransduction. Nonactivated, membrane-associated PDE (PDE-M, $\alpha\beta\gamma_2$) has one exchangeable site for cGMP binding; endogenous cGMP remains nonexchangeable at the second site. Non-activated, soluble PDE (PDE-S, $\alpha\beta\gamma_2\delta$) can release and bind cGMP at both noncatalytic sites; the δ subunit is likely responsible for this difference in cGMP exchange rates. Removal of the δ and/or γ subunits yields a catalytic $\alpha\beta$ dimer with identical catalytic and binding properties for both PDE-M and PDE-S as follows: high affinity cGMP binding is abolished at one site ($K_D > 1 \mu\text{M}$); cGMP binding affinity at the second site ($K_D \sim 60 \text{ nM}$) is reduced 3–4-fold compared with the nonactivated enzyme; the kinetics of cGMP exchange to activated PDE-M and PDE-S are accelerated to similar extents. The properties of nonactivated PDE can be restored upon addition of γ subunit. Occupancy of the noncatalytic sites by cGMP may modulate the interaction of the γ subunit with the $\alpha\beta$ dimer and thereby regulate cytoplasmic cGMP concentration and the lifetime of activated PDE during visual transduction in photoreceptor cells.

The cGMP phosphodiesterase (PDE)¹ present in rod and cone retinal photoreceptors is the central effector enzyme for vertebrate visual excitation. Photoactivation of the visual pigment rhodopsin leads to G-protein (transducin) activation, which then proceeds to the activation of PDE. The activated α subunit of transducin (α_t -GTP) is believed to activate the membrane-associated rod PDE holoenzyme (subunit stoichiometry, $\alpha\beta\gamma_2$) by displacing the inhibitory γ subunits (P γ) from the active sites of the catalytic heterodimer (P $\alpha\beta$). The enhanced hydro-

lytic activity of the activated PDE rapidly reduces cytoplasmic cGMP levels and then leads to dissociation of bound cGMP from the cGMP-gated ion channel, closure of the ion channel, and finally a hyperpolarization of the membrane. These steps constitute the excitation pathway for vertebrate visual transduction (for reviews see Refs. 1–3).

The photoreceptor PDE is a member of a family of phosphodiesterases that all share the ability to hydrolyze cyclic nucleotides. The PDE in rods and cones (classified as PDE6 (4)) is most closely related to the cGMP-specific PDE (PDE5) based on several criteria, including overall amino acid sequence similarity, substrate preference for cGMP over cAMP, inhibition of catalysis by isozyme-selective drugs, and the presence of a consensus sequence in the N-terminal half of the protein that represents noncatalytic cGMP binding domains. In the case of PDE5, binding of cGMP to the noncatalytic cGMP-binding sites may regulate activity indirectly via protein phosphorylation of the enzyme (reviewed in Ref. 5). The cGMP-stimulated PDE (PDE2) also contains noncatalytic cGMP-binding sites that allosterically regulate catalysis at the active site (6).

For the photoreceptor PDE, most of our current knowledge about the role of the noncatalytic sites in PDE regulation has been obtained with amphibian rod PDE. It has been found that cGMP occupancy at the noncatalytic binding sites of frog photoreceptor PDE enhances the association of P γ with P $\alpha\beta$ in a reciprocal manner, and it has been postulated that cGMP binding at the noncatalytic binding sites may determine whether the P γ subunit can participate as an accessory GTPase-activating protein for accelerating transducin inactivation (7–10). In addition, the noncatalytic sites on frog rod PDE have been postulated to serve as a cytoplasmic buffer for cGMP, possibly serving to help restore cGMP levels during recovery from the light stimulation (11, 12).

Much less is known about the function of noncatalytic cGMP-binding sites on photoreceptor PDE during visual transduction in mammalian rod photoreceptors. Two distinct isoforms of rod PDE have been described in bovine rod photoreceptors, a membrane-associated PDE (PDE-M) and a soluble PDE (PDE-S) (13, 14). The only known difference between the two isoforms is the presence of a 17-kDa δ subunit (P δ) associated with PDE-S but not PDE-M (14). The P δ subunit can solubilize membrane-associated PDE *in vitro* (15), but its role in visual transduction has not been determined. The noncatalytic cGMP-binding sites on bovine PDE-M have been shown to bind and release cGMP very slowly (16), and little is known about the cGMP binding properties of PDE-S. Thus, it remains unclear whether the noncatalytic sites on mammalian rod PDE play a similar physiological role to what has been proposed for the amphibian system.

In this paper, we first show that PDE-M and PDE-S in their

* This work was supported by National Institutes of Health Grants EY-05798 (to R. H. C.) and EY-08197 (to J. A. B.). This paper is Scientific Contribution 1994 from the New Hampshire Agricultural Experiment Station. The costs of publication of this article were defrayed in part by the payment of page charges. This article must therefore be hereby marked "advertisement" in accordance with 18 U.S.C. Section 1734 solely to indicate this fact.

¶ To whom correspondence should be addressed: Dept. of Biochemistry and Molecular Biology, University of New Hampshire, 46 College Rd., Durham, NH 03824-3544. Tel.: 603-862-2458; Fax: 603-862-4013; E-mail: Rick.Cote@unh.edu.

¹ The abbreviations used are: PDE, photoreceptor phosphodiesterase; PDE-M, membrane-associated bovine rod PDE; PDE-S, soluble bovine rod PDE; nPDE, non-activated PDE; tPDE, trypsinized PDE; P $\alpha\beta$, catalytic dimer of PDE; P γ , inhibitory 10 kDa γ subunit of PDE; P δ , 17-kDa δ subunit associated with PDE-S; MOPS, 4-morpholinepropane-sulfonic acid.

nonactivated states have different cGMP binding properties. Both high affinity cGMP sites on PDE-S are slowly exchangeable, whereas PDE-M contains one exchangeable and one non-exchangeable noncatalytic site. The presence of the P δ subunit in PDE-S suggests a role for this subunit in enhancing cGMP exchange at one noncatalytic site that is nonexchangeable in PDE-M. Second, activation of the two isoforms leads to similar behavior of PDE-S and PDE-M in terms of the following: 1) a large decrease in cGMP binding affinity at one noncatalytic site; 2) a \sim 10-fold acceleration of cGMP exchange at the remaining high affinity site; and 3) similar hydrolytic rates at the active site. Although it is unlikely that cGMP binding and release at the noncatalytic sites regulate PDE activity during the early events of visual excitation, changes in cGMP occupancy at the noncatalytic sites may help regulate the lifetime of activated PDE during later stages of the visual transduction pathway.

EXPERIMENTAL PROCEDURES

Materials—Bovine retinas were purchased from W. L. Lawson, Inc. Radiochemicals were obtained from NEN Life Sciences Products, and scintillation fluid (Ultima Gold) was from Packard Instrument Co. Zaprinast was a gift of Rhone-Poulenc Rorer (Dagenham, UK). Sulfolink-coupling gel was obtained from Pierce. Pefabloc was obtained from Roche Molecular Biochemicals. cGMP antisera for radioimmunoassays were purchased from Chemicon. Filtration and ultrafiltration products were from Millipore. Superdex 200 and Mono Q columns and pGEX-2T vector and glutathione-Sepharose 4B were from Amersham Pharmacia Biotech. The thrombin cleavage capture kit was from Novagen. The reverse-phase columns for P γ purification were from Vydac. Electrophoretic reagents and immunochemicals were from Bio-Rad. All other chemicals were obtained from Sigma.

Preparation of Nonactivated PDE-S (nPDE-S) and PDE-M (nPDE-M)—Both PDE-S and PDE-M were first partially purified from frozen bovine retinas by modifications of the ion exchange and immunoaffinity chromatography procedures described previously (14, 16, 17). Under infrared illumination, thawed retinas were stirred in a beaker containing 1.5 ml per retina of ROS Buffer (60 mM KCl, 30 mM NaCl, 2 mM MgCl₂, 20 mM MOPS, 1 mM dithiothreitol, 0.2 mM phenylmethylsulfonyl fluoride, pH 7.2) containing 47.5% (w/v) sucrose. The retinal homogenate was centrifuged for 1 h at 8,000 \times g (4 °C), and the supernatant (containing both membrane-associated and soluble PDE isozymes) was removed from the pellet. The pellet was homogenized in 0.4 ml of ROS Buffer per retina to extract additional soluble PDE isozymes and was then centrifuged at 96,000 \times g for 45 min at 4 °C. The supernatant resulting from this spin was pooled with the soluble PDE isozymes obtained below.

The sucrose-containing supernatant from the first centrifugation was diluted 2-fold with ROS Buffer and then centrifuged (23,000 \times g for 45 min at 4 °C). The pellet contained crude ROS which were used to extract PDE-M. The supernatant of this spin (containing soluble PDE isozymes) was combined with the other soluble PDE-containing supernatant. DE52 anion exchange chromatography was employed to separate cone PDE from PDE-S, essentially as described by Gillespie and Beavo (17). PDE-S was further purified by immunoaffinity chromatography using the monoclonal antibody ROS1 (18) immobilized on a Sulfolink-agarose gel.

The crude ROS pellet (containing PDE-M) was resuspended in ROS Buffer, homogenized, and centrifuged at 27,000 \times g for 45 min at 4 °C to remove soluble proteins. After repeating this isotonic washing and centrifugation of the ROS membranes twice, the ROS membranes were exposed to light at 4 °C. PDE-M was extracted four times from the ROS membranes by the following sequence: 1) resuspension and homogenization of the ROS membrane pellet in 0.5 ml/retina of 10 mM Tris, 1 mM MgCl₂, 1 mM dithiothreitol, 0.2 mM phenylmethylsulfonyl fluoride, pH 7.5; 2) centrifugation at 96,000 \times g for 45 min at 4 °C; 3) collection of the PDE-M-containing supernatant. Immunoaffinity purification of the hypothetically extracted PDE-M was then performed.

Immunopurified PDE (PDE purity, \sim 80%) was concentrated in a Centricon concentrator and placed in storage buffer (100 mM NaCl, 2 mM MgCl₂, 10 mM Tris, 2 mM dithiothreitol, 0.4 mM Pefabloc, pH 7.5) containing 50% glycerol at -20 °C. Both PDE-S and PDE-M were further purified by gel filtration chromatography on a Superdex 200 HR 10/30 column equilibrated with Buffer A (120 mM NaCl, 5 mM MgCl₂, 25 mM HEPES, pH 7.5, 2 mM dithiothreitol, 0.2 mM Pefabloc). After elu-

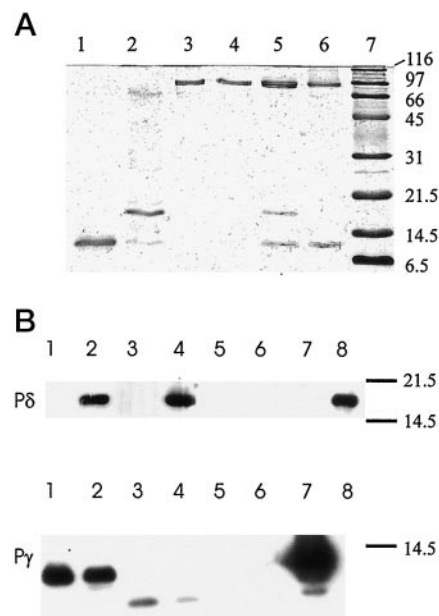


FIG. 1. Purity and subunit composition of nonactivated and trypsin-activated PDE-M and PDE-S enzymes used in this study.

A, 15% SDS-polyacrylamide gels stained with Coomassie Blue. Purity of proteins analyzed was \geq 90% except where noted. *Lane 1*, recombinant bovine P γ (0.42 nmol); *lane 2*, recombinant bovine P δ (2.5 μ g; \sim 80% purity); *lane 3*, purified P $\alpha\beta$ -S (80 pmol); *lane 4*, purified P $\alpha\beta$ -M (80 pmol); *lane 5*, nPDE-S (120 pmol); *lane 6*, nPDE-M (80 pmol); *lane 7*, molecular mass markers (in kDa). **B**, immunoblot analysis using P δ antibody 17K-II (*upper panel*) or P γ antibody UNH9710-4P (*lower panel*). In *lanes 1–6*, 1 pmol of the indicated enzyme was loaded. *Lane 1*, nPDE-M; *lane 2*, nPDE-S; *lane 3*, tPDE-M after concentration but prior to gel filtration, showing an immunoreactive 4.5-kDa P γ proteolytic product; *lane 4*, tPDE-S before concentration or purification, showing undegraded P δ immunoreactivity and a 4.5-kDa P γ peptide; *lane 5*, purified P $\alpha\beta$ -M; *lane 6*, purified P $\alpha\beta$ -S; *lane 7*, P γ (6 pmol); *lane 8*, P δ (20 ng). *Bars*, molecular mass markers.

tion, the purified PDE was concentrated and stored as described above. SDS-polyacrylamide gel electrophoresis of the purified, non-activated PDE-S (nPDE-S) and non-activated PDE-M (nPDE-M, Fig. 1A, *lanes 5 and 6*, respectively) shows that $>$ 90% of the Coomassie-stained bands represent the catalytic and low molecular weight subunits of PDE. For five different purified PDE preparations, we recovered 2.6 ± 1.1 nmol of purified nPDE-M and 1.0 ± 0.4 nmol of nPDE-S per 100 bovine retinas using these procedures.

Preparation of Trypsinized PDE-M (tPDE-M) and PDE-S (tPDE-S)—To prepare P $\alpha\beta$ dimers from nPDE-S and from nPDE-M, limited proteolysis with L-1-tosylamido-2-phenylethyl chloromethyl ketone-treated trypsin was performed (13, 19, 20). Purified nPDE (0.8–1.0 mg/ml) was prepared in 25 mM MOPS, pH 7.5, containing 25% glycerol, and incubated at 4 °C with 50 μ g/ml of trypsin for 35–40 min. These conditions were optimized to obtain complete enzyme activation (using a PDE activity assay) without causing the appearance of a 70-kDa proteolytic fragment of the catalytic subunits (as judged by Coomassie-stained SDS-polyacrylamide gels of the trypsinized enzymes (Fig. 1A, *lanes 3 and 4*; see also Refs. 21 and 22)). Proteolysis was halted with a 6-fold weight excess of soybean trypsin inhibitor. Analysis of the trypsinized PDE-S (tPDE-S) preparation at this stage showed that the P δ subunit was not degraded to a significant extent (Fig. 1B, *lane 4*).

The trypsinized PDE (tPDE) was then diluted $>$ 500-fold into Buffer A to enhance dissociation of the low molecular weight subunits and their proteolytic fragments. Ultrafiltration (BioMax, 30,000 molecular weight cut-off) of the tPDE was performed to concentrate the enzyme. Substantial amounts of an \sim 4,500-kDa band that immunoreacted with the C-terminal P γ polyclonal antibody (UNH9710-4P) remained in the tPDE samples at this stage (Fig. 1B, *lanes 3 and 4*).

To prepare pure P $\alpha\beta$ preparations from the trypsinized enzyme preparations, the tPDE was further purified by Superdex-200 chromatography using Buffer A as the mobile phase. This was followed by anion exchange chromatography on a Mono Q HR 5/5 column equilibrated in 250 mM NaCl, 1 mM MgCl₂, 25 mM Tris, pH 7.5, 1 mM DTT, and 0.2 mM phenylmethylsulfonyl fluoride, using a linear gradient from

250 to 500 mM NaCl to elute $\text{P}\alpha\beta$ dimers. The purity of the $\text{P}\alpha\beta$ -S or $\text{P}\alpha\beta$ -M prepared from tPDE-S or tPDE-M, respectively, was found to be >90% by Coomassie-stained gels (Fig. 1A, lanes 3 and 4), with undetectable levels of $\text{P}\gamma$ or $\text{P}\delta$ immunoreactivity (Fig. 1B, lanes 5 and 6).

Determination of the Catalytic Constant (k_{cat}) for Trypsin-activated PDE—We routinely determined the concentration of native PDE by measuring the maximum hydrolytic activity (V_{max}) of a PDE-containing sample following limited proteolysis to activate fully the enzyme (described above); using activity measurements instead of total protein determinations to estimate the PDE concentration distinguishes native (*i.e.* non-denatured) PDE from denatured enzyme and minor impurities present in our PDE preparations.

To calculate the concentration of enzyme from the equation, $[\text{P}\alpha\beta] = V_{\text{max}}/k_{\text{cat}}$, we needed to accurately determine the catalytic constant (k_{cat}) for our PDE-M and PDE-S preparations. The determination of the k_{cat} required independent knowledge of the PDE concentration, which was obtained by total protein determinations (Bradford method) and by measuring the maximum cGMP-binding site density (B_{max}). The latter approach relies on observations that bovine nPDE-M can bind 2.0 mol of cGMP per mol of catalytic dimer (16) and that tPDE is capable of binding only 1 mol of [^3H]cGMP per mol of catalytic dimer under our conditions (see under "Results"). For the case of PDE-M, the trypsin-activated enzyme has a $k_{\text{cat}} = 5550 \pm 100$ mol of cGMP hydrolyzed per s/mol of [^3H]cGMP bound ($n = 24$) at 22 °C. Trypsin-activated PDE-S is able to hydrolyze 5620 ± 110 mol of cGMP/s/mol of [^3H]cGMP bound ($n = 16$). We have used the average value, $k_{\text{cat}} = 5600$ cGMP hydrolyzed per $\text{P}\alpha\beta$ /s, in our calculations of PDE concentration. This value is $22 \pm 3\%$ ($n = 4$) higher than that obtained in identical PDE-S and PDE-M samples in which the Bradford assay was used to quantitate PDE concentration ($k_{\text{cat}} = 4930$ cGMP hydrolyzed per PDE/s).

Purification of $\text{P}\gamma$ and $\text{P}\delta$ —The recombinant bovine rod $\text{P}\gamma$ subunit was expressed in bacteria as described (23) with the following modifications. Following cation exchange chromatography, $\text{P}\gamma$ was chromatographed on a preparative C18 reverse-phase column (300 Å, 22×250 mm) using a linear gradient of 30–50% acetonitrile in 0.1% trifluoroacetic acid. The purity of the $\text{P}\gamma$ peak was verified on an analytical Vydac C4 reverse-phase column (300 Å, 4.6×25 mm) and by SDS-polyacrylamide gel electrophoresis (Fig. 1A, lane 1). The concentration of $\text{P}\gamma$ was routinely measured spectrophotometrically after having empirically determined the extinction coefficient ($\epsilon_{277} = 7550 \text{ cm}^{-1}$ in 45% acetonitrile, 0.1% trifluoroacetic acid) in conjunction with amino acid analysis. The inhibitory activity of $\text{P}\gamma$ preparations was assessed as described previously (24) and was typically >95% active.

The recombinant $\text{P}\delta$ subunit was expressed and purified by two different methods. In the first method, the $\text{P}\delta$ subunit was overexpressed in Sf9 cells using a baculovirus expression system; the protein was then purified by anion exchange chromatography and ultrafiltration, as described in detail in Florio *et al.* (15). The second method was to subclone the 17K-11 $\text{P}\delta$ coding sequence (15) into the pGEX2T expression vector and to express the $\text{P}\delta$ -GST fusion protein following standard procedures. Following purification on a glutathione-Sepharose affinity column, the fusion partner was cleaved, and the protease was removed with the use of a thrombin cleavage capture kit according to the manufacturer's instructions. The $\text{P}\delta$ was concentrated by ultrafiltration and stored in 50% glycerol at -20 °C. (Upon sequencing the $\text{P}\delta$ -GST construct, a polymerase chain reaction artifact was discovered that caused an amino acid substitution at position 85 from glutamine to arginine. No functional differences could be detected when the cleaved fusion protein containing the substitution was compared with the $\text{P}\delta$ expressed from Sf9 cells.)

The concentration of $\text{P}\delta$ was determined using the Bradford assay. The purity of different $\text{P}\delta$ preparations was found to exceed 80% for both methods (*e.g.* Fig. 1A, lane 2); immunoblot analysis with the 17K-II $\text{P}\delta$ antibody revealed a single immunoreactive band at ~ 17 kDa.

Measurements of cGMP Binding to Noncatalytic Sites on PDE—Two different methods were used to quantitate cGMP binding to the noncatalytic sites on PDE, cGMP radioimmunoassay, and a membrane filtration assay. Purified, concentrated PDE was first diluted in Buffer B (77 mM KCl, 35 mM NaCl, 2.0 mM MgCl_2 , 1.0 mM CaCl_2 , 1.18 mM EGTA ($[\text{Ca}^{2+}]_{\text{free}} = 240 \text{ nM}$), 10 mM HEPES, pH 7.5) supplemented with final concentrations of 1.0 mM dithiothreitol, 0.5 $\mu\text{g/ml}$ leupeptin, 0.2 mM Pefabloc, and 0.7 $\mu\text{g/ml}$ pepstatin. In experiments where depletion of endogenous nucleotides was attempted by incubating the PDE at 37 °C (24 h for nPDE and 2 h for tPDE), Buffer B was supplemented with 5-fold greater concentrations of protease inhibitors and dithiothreitol, as well as 0.1 mg/ml bovine serum albumin and 30% glycerol (to minimize loss of PDE activity (<20% over the 24-h period)); before use, the nucleotide-depleted PDE was diluted >10-fold in Buffer B lacking

the supplements.

To measure the amount of endogenous cGMP remaining bound to PDE following purification, a cGMP radioimmunoassay was used. Briefly, PDE-containing samples were quenched with 50% HCl in ethanol and then centrifuged to remove precipitated material. The acidic supernatant was dried under vacuum, and the neutralized sample was resuspended in 0.1 M citrate, pH 6.2. The radioimmunoassay was performed as described in Cote *et al.* (25), with an operating range of 0.15 to 3 pmol of cGMP per sample, as judged by comparison with a standard curve using known amounts of cGMP treated identically to the unknown samples.

To determine the equilibrium and kinetic properties of [^3H]cGMP binding to the various PDE preparations, a membrane filtration assay was used (26). PDE-containing samples in Buffer B were incubated with the indicated concentrations of [^3H]cGMP in the presence of 0.1 or 0.8 mM zaprinast, a photoreceptor PDE catalytic site inhibitor (27). The higher zaprinast concentration was used with activated PDE samples to ensure that the extent of [^3H]cGMP hydrolysis during the incubation period was <10% under all conditions tested. In separate experiments, we verified that 2–1000 μM zaprinast was unable to compete with [^3H]cGMP bound to the noncatalytic sites of nPDE-M to which excess $\text{P}\gamma$ had been added to prevent ligand hydrolysis.

Following incubation of PDE with the radiolabeled cGMP, portions were directly filtered on prewet nitrocellulose membranes (Millipore HA membrane, 0.45 μm) and quickly (<4 s) rinsed with three 1-ml portions of ice-cold Buffer B. Nonspecific binding was determined as described previously (11). The membrane filtration technique is useful for measuring relatively high affinity ligand binding ($K_D < 1 \mu\text{M}$); lower affinity cGMP-binding sites are likely to release bound cGMP during the washing procedure and may go undetected.

Analytical Procedures—A colorimetric, coupled enzyme assay was employed for measurements of cGMP hydrolytic rates, as described in detail elsewhere (26). SDS-polyacrylamide gel electrophoresis followed the procedure of Laemmli (28). Immunoblot analyses of the $\text{P}\gamma$ and $\text{P}\delta$ subunits were performed with polyclonal antiserum UNH9710-4P to the C-terminal region (amino acids 63–87) of $\text{P}\gamma$ or antiserum 17K-II to residues 23–41 of the $\text{P}\delta$ protein (15) along with a goat anti-rabbit secondary antibody coupled to horseradish peroxidase, using standard protocols (29). Protein concentrations were estimated with the Bradford assay (30) using bovine serum albumin as a standard; a correction factor of 1.2 was applied for estimates of purified PDE catalytic subunit concentrations (16). Data analysis was performed using Sigmaplot (SPSS, Inc.) and KELL (Biosoft). All experiments were repeated at least three times, and error estimates represent the S.E.

RESULTS

The Soluble and Membrane-associated Isoforms of Bovine Rod PDE Have Different cGMP Binding Properties in Their Nonactivated States—As reported previously, the nonactivated, membrane-associated PDE (nPDE-M, $\alpha\beta\gamma_2$) of bovine rod photoreceptors binds 2 mol of cGMP per mol of PDE very tightly and exchanges its bound cGMP very slowly (16). To compare directly the cGMP binding properties of the soluble PDE (nPDE-S, $\alpha\beta\gamma_2\delta$) with nPDE-M, we measured both the amount of endogenous cGMP remaining bound to purified, nonactivated PDE (nPDE) by cGMP radioimmunoassay, and the amount of exchangeable [^3H]cGMP-binding sites by a membrane filtration assay (see "Experimental Procedures"). For the case of the membrane-associated isoform, we found that purified nPDE-M retained 1.9 ± 0.04 mol of cGMP per PDE of holoenzyme ($\alpha\beta\gamma_2$) as judged by a cGMP radioimmunoassay (Fig. 2). Approximately 0.1 ± 0.04 mol of [^3H]cGMP was able to bind to nPDE-M in this condition. These results are identical to previous measurements where tightly bound, endogenous cGMP (1.8 ± 0.3 mol of cGMP/PDE) as well as [^3H]cGMP binding (0.1 mol of cGMP/PDE) were analyzed by high pressure liquid chromatography (16). Incubation of nPDE-M for 24 h at 37 °C resulted in the loss of 1 mol of endogenous cGMP per PDE with the concomitant ability to bind 1 mol of [^3H]cGMP per PDE (Fig. 2). We conclude that nPDE-M consists of 2 high affinity, noncatalytic cGMP-binding sites, of which only one is able to release its bound cGMP under these conditions.

The nonactivated, soluble isoform of rod PDE (nPDE-S) also

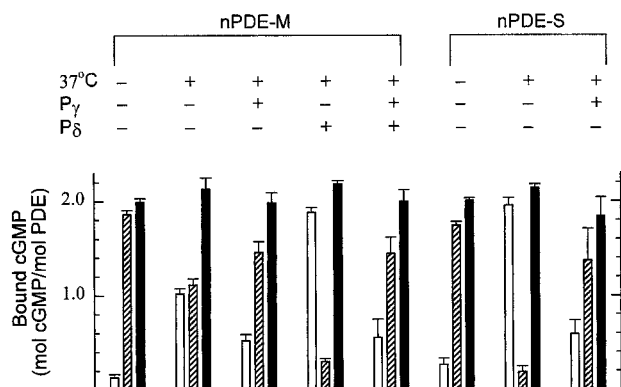


FIG. 2. Effects of temperature and added P γ and P δ subunits on the noncatalytic cGMP-binding sites of nPDE-M and nPDE-S. Purified nPDE-M and nPDE-S were diluted to 50 nM concentration in Buffer B (containing the higher levels of supplements, including 30% glycerol and 0.1 mg/ml bovine serum albumin as stabilizers), as described under "Experimental Procedures." The PDE samples were then incubated under the following conditions, as indicated in the heading: -37°C, 24 h at 4°C; +37°C, 24 h at 37°C; +P γ , addition of 10 mol of P γ /mol of P $\alpha\beta$ to PDE at onset of 37°C incubation; +P δ , addition of 5 mol of P δ /mol of P $\alpha\beta$ at onset of 37°C incubation. After the incubation period, portions were removed for analysis of endogenous cGMP remaining bound by cGMP radioimmunoassay (hatched bars). Other portions were incubated with 1 μ M [³H]cGMP for 30 min at 4°C, and then membrane filtration was performed (open bars). The y axis is expressed as mol of cGMP bound per mol of PDE holoenzyme for each assay, as well as the sum of the endogenous and [³H]cGMP binding (filled bars).

retains bound endogenous cGMP following its extensive purification (1.7 ± 0.04 mol cGMP/mol PDE; Fig. 2). Upon addition of exogenous [³H]cGMP, the total binding stoichiometry is 2.0 ± 0.1 mol of cGMP/mol of PDE, identical to nPDE-M. One major difference between nPDE-M and nPDE-S is the ability of the soluble isoform to release ~90% of its endogenous cGMP upon 24 h incubation at 37°C, as well as being able to bind 1.9 ± 0.08 mol of [³H]cGMP/PDE. We conclude that both high affinity noncatalytic binding sites on nPDE-S are able to undergo nucleotide exchange, whereas only one site is exchangeable in nPDE-M.

One obvious difference between nPDE-M and nPDE-S is the presence of the P δ subunit associated with nPDE-S. To test whether the P δ subunit could account for the different cGMP binding properties noted above, we incubated nPDE-M with an excess of recombinant P δ subunit. As shown in Fig. 2, incubation with P δ can cause the release of endogenous cGMP from the formerly "nonexchangeable" binding site on nPDE-M; only 0.3 ± 0.03 mol of cGMP/mol of PDE remain bound after a 24-h incubation at 37°C, whereas addition of [³H]cGMP to the nucleotide-depleted enzyme permits 1.9 ± 0.05 mol of cGMP/mol of PDE to bind. This result indicates that P δ can bind to nPDE-M (in accord with a previous reconstitution study (15)) and enhance the rate of cGMP exchange at one of the noncatalytic cGMP-binding sites that is essentially nonexchangeable when P δ is absent.

We also examined the effects of adding a 10-fold molar excess of P γ on the cGMP binding properties of nPDE-M and nPDE-S. In all cases where P γ was added, the amount of endogenous cGMP that was retained following the 24-h incubation was increased to ~1.4 mol of cGMP/mol of PDE, regardless of whether the P δ subunit was also added in molar excess (Fig. 2). The ability of [³H]cGMP to bind was reduced in a corresponding manner (~0.5–0.6 mol of [³H]cGMP/mol of PDE) for both nPDE-M and nPDE-S. We conclude that the P γ subunit acts to reduce the rate of cGMP dissociation from exchangeable noncatalytic sites on both nPDE-M and nPDE-S.

Activation of PDE by Limited Proteolysis of the P γ Subunit

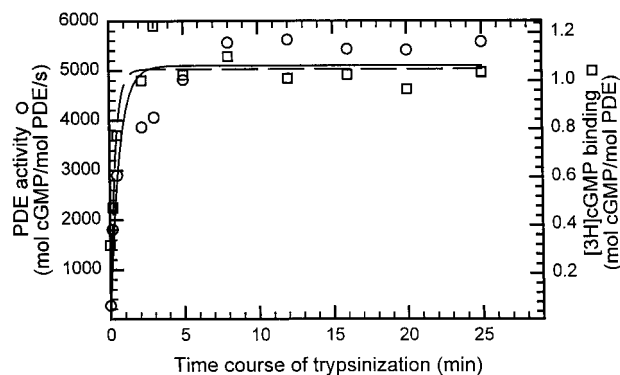


FIG. 3. Activation of nPDE-S by limited proteolysis follows the same time course as ability to bind [³H]cGMP to one noncatalytic site on PDE. Purified nPDE-S was incubated with trypsin (45 μ g/ml) at 4°C as described under "Experimental Procedures." At the indicated times, portions were treated with soybean trypsin inhibitor to stop proteolysis, and the tPDE-S (590 nM) was then incubated at 37°C for 30 min to permit release and degradation of any rapidly exchangeable cGMP. The enzymatic activity (using 2 mM cGMP as substrate, circles) or the ability to bind 1 μ M [³H]cGMP (5 min at 37°C to minimize binding to non-activated sites, squares) was determined as described under "Experimental Procedures." These data points are from one of three representative experiments, and the curves represent a fit to a single exponential model.

Alters the cGMP Binding Properties of PDE—Since addition of P γ reduces the amount of endogenous cGMP released as well as the amount of [³H]cGMP that could associate with the noncatalytic sites of nPDE-M or nPDE-S (Fig. 2), we reasoned that removal of the P γ subunits from the holoenzyme would enhance the ability of cGMP to exchange between the bound and free state. To test this, we exposed a preparation of purified nPDE-S to mild trypsin proteolysis (20) for various times at 4°C. As described under "Experimental Procedures," this treatment degrades the P γ subunit and relieves inhibition of catalysis at the active site, with no detectable effect on the apparent molecular weights of P δ or P $\alpha\beta$ on SDS-polyacrylamide gels (Fig. 1). We then measured the ability of 1 μ M [³H]cGMP to occupy the noncatalytic sites, as well as the maximum hydrolytic rate of tPDE-S. Fig. 3 shows that the time course of activation by trypsin correlated well with the ability to bind up to 1 mol of [³H]cGMP per catalytic dimer. (Identical trypsin time course experiments performed on nPDE-M gave essentially identical results to those shown for nPDE-S in Fig. 3 (data not shown).) Separate measurements by radioimmunoassay of the endogenous cGMP remaining bound to fully activated tPDE-S at the time when the [³H]cGMP was added (<0.3 cGMP/PDE) indicated that >85% of the total bound cGMP had dissociated and been degraded by the activated enzyme. Therefore, the inability to bind more than 1 mol of cGMP per mol of PDE could not be due to endogenous bound cGMP preventing [³H]cGMP association. One possible conclusion from this result is that the proteolytic destruction of P γ had lowered (below the level of detection by membrane filtration) the binding affinity for cGMP at only one of the two noncatalytic sites. Another possibility we considered was that trypsin had damaged the catalytic subunits so that high affinity cGMP binding at one of the noncatalytic sites was permanently lost.

To distinguish these possibilities, we prepared purified catalytic dimers of PDE-S (P $\alpha\beta$ -S) from which all traces of the low molecular weight subunits had been removed (see "Experimental Procedures" and Fig. 1); this P $\alpha\beta$ -S preparation also lacked detectable amounts of endogenous cGMP at the noncatalytic sites. Purified P $\alpha\beta$ -S was able to bind 1 mol of cGMP per mol of PDE in the absence of P γ , in agreement with the results with tPDE-S in Fig. 3. Following addition of increasing amounts of

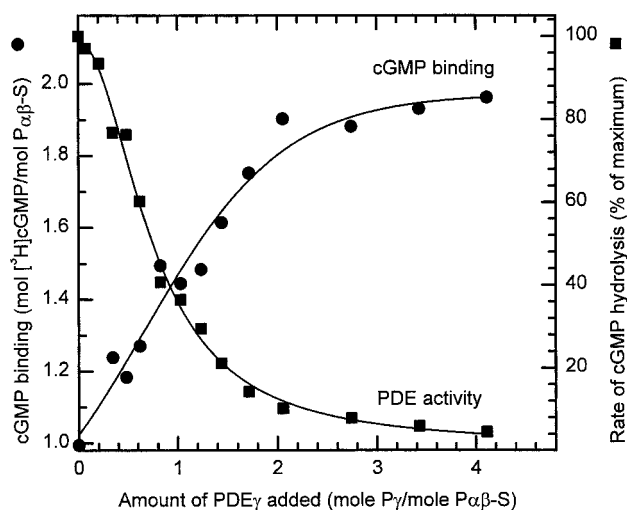


FIG. 4. Addition of stoichiometric amounts of $P\gamma$ is sufficient to restore cGMP binding to the second high affinity noncatalytic binding site of $P\alpha\beta$ -S. Purified $P\alpha\beta$ -S was first depleted of endogenous cGMP by incubation at 37 °C (<0.1 mol of cGMP bound/mol of $P\alpha\beta$ -S), as described under "Experimental Procedures." The indicated amounts of purified $P\gamma$ were incubated with $P\alpha\beta$ -S for 30 min at 4 °C prior to commencing activity (1.4 nM PDE) and binding assays (5 nM PDE). The hydrolytic activity was measured with 10 mM cGMP as substrate and normalized to the rate in the absence of added $P\gamma$ (5240 mol of cGMP hydrolyzed per mol of PDE/s). 1 μ M [3 H]cGMP was incubated for 30 min at 37 °C prior to filter binding. The symbols represent individual data points from one of three similar experiments.

$P\gamma$ to $P\alpha\beta$ -S, we observed a progressive increase in [3 H]cGMP binding that correlated with the inhibition of hydrolysis at the active site (Fig. 4). Addition of 2 mol of $P\gamma$ per mol of $P\alpha\beta$ -S permitted an additional 0.9 mol of [3 H]cGMP per mol of $P\alpha\beta$ -S to bind and inhibited 90% of the hydrolytic activity of the enzyme. (Identical results were obtained upon titration of $P\alpha\beta$ -M with $P\gamma$ (data not shown).) In none of our experiments did we detect an effect of adding $P\delta$ on cGMP binding to high affinity sites on $P\alpha\beta$ -S or $P\alpha\beta$ -M.

Several interesting conclusions can be drawn from the above results. First, purified $P\alpha\beta$ dimers derived from PDE-S and PDE-M are able to bind 1 mol of cGMP per $P\alpha\beta$ in the complete absence of $P\gamma$, $P\delta$, or their proteolytic fragments. Second, it follows that removal of $P\gamma$ from PDE reduces the binding affinity of cGMP for one of the two noncatalytic sites below the level of detection of binding assay ($K_D > 1 \mu$ M). Third, the proteolytic treatment of $P\alpha\beta$ is reversible upon addition of stoichiometric amounts of $P\gamma$. This shows that the $P\gamma$ subunit is the major target of action of trypsin and that the limited proteolysis does not destroy the ability of $P\alpha\beta$ to bind cGMP at the "low affinity" site if $P\gamma$ is added back. Finally, in contrast to the two non-identical cGMP-binding sites on $P\alpha\beta$, no difference in binding affinity of $P\gamma$ to the two $P\gamma$ -binding sites on $P\alpha\beta$ could be discerned for either PDE-S or PDE-M. We infer this from the observation that addition of 1 $P\gamma$ per $P\alpha\beta$ restores approximately one-half of the total cGMP binding that requires $P\gamma$ binding to $P\alpha\beta$.

Kinetic and Equilibrium Analysis of cGMP Binding to Noncatalytic Sites on PDE-S and PDE-M—To understand better the regulation of cGMP binding at the two non-identical binding sites on the soluble and membrane-associated rod PDE isoforms, we analyzed the kinetics and equilibrium binding of cGMP to both nPDE and $P\alpha\beta$ preparations for both PDE-S and PDE-M. Equilibrium binding measurements were performed at 37 °C over the range of 2 to 400 nM cGMP for each PDE preparation, and the K_D and B_{\max} values were determined (Fig. 5; see Table I for average values from several experiments). In

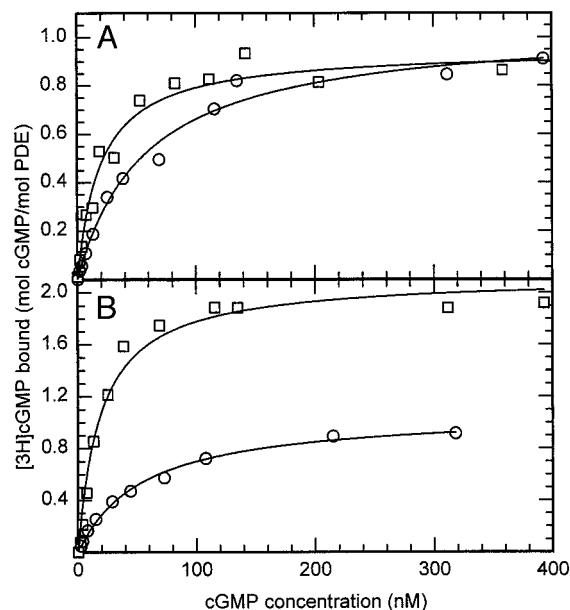


FIG. 5. Equilibrium binding of cGMP to nonactivated and activated rod PDE isoforms. Purified PDE preparations were first incubated at 37 °C to remove exchangeable, bound cGMP, as described under "Experimental Procedures." Except for nPDE-M (~ 1 mol of endogenous cGMP bound/mol of PDE), each PDE preparation retained <0.1 mol of endogenous cGMP/mol of PDE following nucleotide depletion. Each preparation was diluted to 5 nM (final concentration) in Buffer B and was incubated with the indicated concentrations of [3 H]cGMP at 37 °C for 30 min prior to membrane filtration. Curves represent the fit to a single-site binding model. A, binding of nPDE-M (squares), $K_D = 20$ nM, and $B_{\max} = 0.95$ mol of cGMP/mol of PDE; binding to $P\alpha\beta$ -M (circles), $K_D = 58$ nM and $B_{\max} = 1.04$ mol of cGMP/mol of PDE. B, binding of nPDE-S (squares), $K_D = 19$ nM, $B_{\max} = 2.12$ mol of cGMP/mol of PDE; binding to $P\alpha\beta$ -S (circles), $K_D = 54$ nM and $B_{\max} = 1.08$ mol cGMP/mol PDE. The symbols represent individual data points from a single experiment; see Table I for average values for n determinations.

all cases, the equilibrium binding data fit a model for a single class of non-interacting binding sites, even in the case of nPDE-S where the stoichiometry of binding indicated 2 binding sites per holoenzyme (Table I). For the case of PDE-S, limited trypsin proteolysis of the enzyme resulted in the loss of detectable cGMP binding at one of the noncatalytic sites, and a 4-fold reduction in cGMP binding affinity at the remaining site. For the case of nPDE-M where only one site is available to exchange cGMP (the other retaining bound endogenous cGMP; Fig. 2), trypsinization reduces the binding affinity 3-fold; note, however, that we cannot distinguish whether the exchangeable or nonexchangeable site is responsible for the cGMP binding we detect in activated $P\alpha\beta$ -M.

It is evident from comparing the K_D values of the two isoforms that the single exchangeable noncatalytic binding site we detect in nPDE-M has the same binding affinity for cGMP as the 2 sites that bind [3 H]cGMP in nPDE-S. Likewise, trypsin activation of each isoform results in a loss of detectable binding to one of the two cGMP-binding sites per $P\alpha\beta$, and a uniform decrease in binding affinity ($K_D \sim 60$ nM) of cGMP at the other site. These results strongly suggest that PDE-M and PDE-S have very similar or identical cGMP-binding sites on the $P\alpha\beta$ dimer. Furthermore, association of $P\gamma$ and $P\delta$ with $P\alpha\beta$ each have distinct effects in modulating cGMP binding to the two noncatalytic sites of PDE.

Kinetic analysis of the association and dissociation kinetics of cGMP binding to PDE provides an additional approach for understanding how cGMP binding to the noncatalytic sites is regulated. Fig. 6 shows that when the $P\gamma$ and $P\delta$ subunits are removed from the catalytic dimer to form $P\alpha\beta$ -S, both the

TABLE I
Comparison of the [^3H]cGMP binding properties of bovine rod PDE isoforms

The experimental conditions for the equilibrium binding measurements and the kinetics measurements are provided in the legends to Figs. 5 and 6, respectively. The data represent the mean (\pm S.E.); the value in parentheses is the number of independent determinations.

PDE ^a	Maximum [^3H]cGMP binding (cGMP/PDE)	Measured K_D	Dissociation kinetics, k_{-1}		Association kinetics, k_{+1}		Kinetic $K_D = k_{-1}/k_{+1}$ ^b
			<i>nM</i>	<i>s</i> ⁻¹	<i>M</i> ⁻¹ <i>s</i>	<i>nM</i>	
nPDE-M ^c	1.00 \pm 0.04 (3)	18 \pm 2 (3)	3.9 \pm 0.1 \times 10 ⁻⁴ (3)	2.2 \pm 0.6 \times 10 ⁴ (4)		18	
P $\alpha\beta$ -M	1.02 \pm 0.04 (4)	56 \pm 4 (4)	6.8 \pm 1.0 \times 10 ⁻³ (5)	9.8 \pm 1.9 \times 10 ⁴ (8)		71	
nPDE-S	1.85 \pm 0.09 (4)	14 \pm 2 (4)	4.5 \pm 0.9 \times 10 ⁻⁴ (5)	2.3 \pm 0.4 \times 10 ⁴ (4)		20	
P $\alpha\beta$ -S	0.93 \pm 0.03 (3)	57 \pm 13 (3)	7.2 \pm 0.4 \times 10 ⁻³ (5)	1.3 \pm 0.2 \times 10 ⁵ (4)		55	

^a nPDE refers to PDE holoenzyme containing the low molecular subunits; P $\alpha\beta$ refers to activated PDE catalytic dimer lacking P γ and/or P δ . The -M and -S suffix refer to membrane-associated and soluble forms of PDE, respectively.

^b The kinetic K_D is in general agreement with the measured K_D , indicating the internal consistency of the equilibrium binding and kinetic data.

^c nPDE-M has one nonexchangeable site (Fig. 2) that cannot be detected in these experiments.

association and dissociation rates of cGMP with the one remaining high affinity noncatalytic site are accelerated. The association rate constant (k_{+1}) is increased 6-fold upon removal of P γ and P δ from P $\alpha\beta$ -S, whereas the dissociation rate constant (k_{-1}) increases 16-fold (Table I). Kinetic analyses of the noncatalytic sites on PDE-M (Table I) are in general agreement with the results obtained with PDE-S. Upon removal of P γ , the k_{+1} of P $\alpha\beta$ -M for the one high affinity binding site is increased 4-fold compared with nPDE-M, whereas the k_{-1} is increased 17-fold by P γ removal. The similar kinetic behavior of PDE-M and PDE-S indicates that the binding of P γ (rather than P δ) is the major factor affecting the ability of cGMP to bind to and dissociate from the noncatalytic sites on both PDE-S and PDE-M. Furthermore, the interaction of P γ with P $\alpha\beta$ has its greatest effect on the cGMP dissociation rate constant, rather than the k_{+1} or the K_D . This is intriguing since it is the rate of cGMP dissociation from noncatalytic sites on PDE that is most relevant to proposed physiological roles of these sites in regulating PDE during recovery or light adaptation (see under "Discussion").

Although we cannot measure detectable [^3H]cGMP binding to the second noncatalytic site on P $\alpha\beta$ with our filter binding assay, some minimum values of the binding parameters can be inferred. The time required for filtration (\sim 4 s) sets a limit to highest dissociation rate constant that can be measured (26). Since the half-time for cGMP dissociation from the higher affinity site on P $\alpha\beta$ -S or P $\alpha\beta$ -M is \sim 100 s (Table I), the lower affinity site must have a dissociation rate at least 25-fold larger in order for any bound cGMP to be released (and therefore not detected) during the filtration process. This implies that the K_D for the lower affinity site is likely to be $>$ 25-fold larger ($>$ 1.5 μM) than the value measured for P $\alpha\beta$ -S and P $\alpha\beta$ -M. We conclude that activation of PDE reduces the binding affinity at one site only 3–4-fold, whereas the other binding site undergoes a $>$ 25-fold reduction in affinity with a concomitant acceleration of the cGMP dissociation rate.

DISCUSSION

We have shown that mammalian rod photoreceptor PDE isoforms can undergo substantial changes in cGMP binding to two non-identical, high affinity noncatalytic sites upon activation of the enzyme by removal of the P γ subunits. We also report that the soluble and membrane-associated isoforms of bovine rod PDE have different binding properties in their non-activated states. Finally, our results demonstrate that the P γ subunit is primarily responsible for altering cGMP exchange upon activation and that the P δ subunit may interact with P γ binding to the enzyme to permit cGMP exchange at a site on non-activated PDE that is nonexchangeable in PDE-M but exchangeable in PDE-S.

The Two High Affinity Noncatalytic Binding Sites on Bovine Rod PDE Are Not Identical—Previous work established that the PDE-M holoenzyme contains 2 high affinity cGMP-binding

sites that retain bound cGMP even following extensive purification (16). We have extended that work to demonstrate that the soluble isoform of rod PDE also contains 2 high affinity cGMP-binding sites. Of greater significance is the demonstration that the two noncatalytic sites are not identical in their cGMP binding properties. The presence of one functionally nonexchangeable cGMP-binding site on nonactivated PDE-M is in marked contrast to the two exchangeable sites found in bovine rod PDE-S (Fig. 2), cone PDE (17), or the amphibian membrane-associated rod PDE (10).

Activation of bovine rod PDE reveals a fundamental difference between the two non-identical noncatalytic sites on both bovine rod isoforms. Removal of the P γ subunits from PDE-M or PDE-S eliminates detectable binding ($K_D > 1 \mu\text{M}$) of cGMP to one of the two classes of noncatalytic sites on the P $\alpha\beta$ dimer. This effect represents a shift of \geq 100-fold in overall cGMP binding affinity at this site and a rate of dissociation that is too fast to detect by filter binding ($t_{1/2} < 4$ s). The remaining cGMP-binding sites exhibit a 3-fold reduction in overall binding affinity upon removal of P γ compared with the [^3H]cGMP-binding sites on nPDE-M or nPDE-S. We conclude that the P γ subunit not only acts in its well known role as an inhibitor of cyclic nucleotide catalysis at the active sites on P $\alpha\beta$ but also serves to regulate the affinity of interaction of cGMP with the two distinct noncatalytic sites on the P $\alpha\beta$ dimer. The amphibian PDE, in contrast, shows no detectable cGMP binding to P $\alpha\beta$ when the P γ subunits are removed by limited proteolysis (7, 8) or by extraction with activated transducin (10).

No Intrinsic Differences in the Catalytic P $\alpha\beta$ Dimers Derived from PDE-S and PDE-M—Based on the results of this study and previous work (14, 15), it appears very likely that the catalytic subunits are identical in PDE-S and PDE-M. The molecular weights of α and β are indistinguishable on SDS-polyacrylamide gels (14), and the catalytic constant of tPDE-S is identical to that of tPDE-M (see "Experimental Procedures" and Ref. 14), and the noncatalytic cGMP-binding sites show very similar kinetic and equilibrium binding behavior for the purified P $\alpha\beta$ dimers derived from PDE-S and PDE-M (Figs. 5–6 and Table I). Whereas a definitive statement awaits direct amino acid sequence comparisons of the α and β subunits of PDE-S and PDE-M, all available evidence indicates that binding of the P δ subunit to the PDE holoenzyme confers the differences in behavior seen with nPDE-S and nPDE-M.

Two Distinct Actions of P δ on PDE—We report a new function that can be ascribed to the binding of the P δ subunit to rod PDE; the ability of P δ to permit cGMP release from a second noncatalytic binding site on nPDE-S that remains functionally nonexchangeable in PDE-M. How this effect of P δ on PDE-S relates to the other known function of P δ (namely to solubilize PDE that would otherwise remain attached to rod outer segment disk membranes (15)) is not clear at present. However, membrane association of PDE is not required for P δ binding,

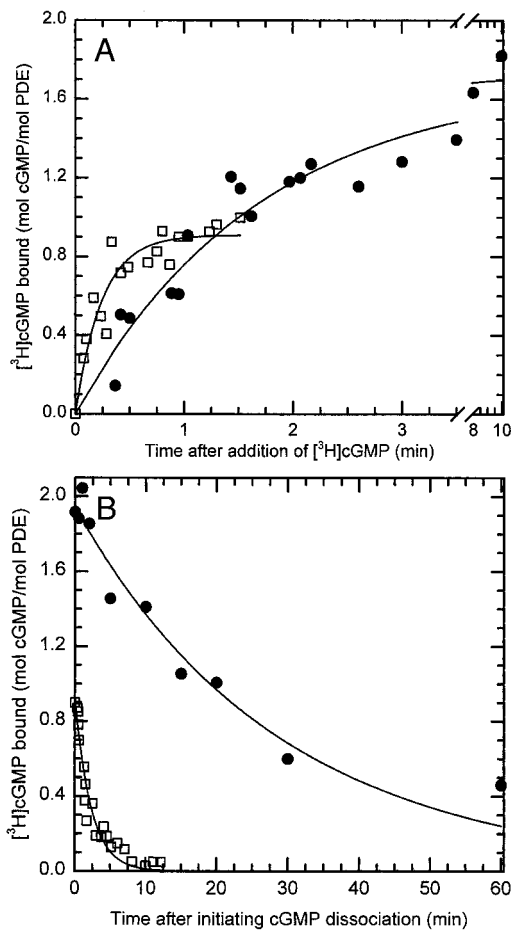


FIG. 6. The kinetics of cGMP association and dissociation to PDE-S are accelerated upon enzyme activation. Purified nPDE-S and P $\alpha\beta$ -S were depleted of their endogenous nucleotides by incubation at 37°C for 16 and 2 h, respectively. A, association kinetics were obtained at 37°C by adding ~ 500 nM $[^3\text{H}]$ cGMP to 8 nM nPDE-S (circles) or P $\alpha\beta$ -S (squares) at time 0 and filtering samples at the indicated times. The data were analyzed as a pseudo-first order reaction with the association rate constant $k_{+1} = (k_{\text{obs}} - k_{-1})/[\text{cGMP}]_{\text{tot}}$, where k_{obs} is the first-order rate constant for the single exponential, k_{-1} is the dissociation rate constant (determined in B), and $[\text{cGMP}]_{\text{tot}}$ is the total $[^3\text{H}]$ cGMP concentration. The data fit a single exponential function for both nPDE-S ($k_{\text{obs}} = 9.8 \pm 1.0 \times 10^{-3} \text{ s}^{-1}$; $B_{\text{max}} = 1.7 \pm 0.1$ $[^3\text{H}]$ cGMP bound/PDE) and P $\alpha\beta$ -S ($k_{\text{obs}} = 0.068 \pm 0.011 \text{ s}^{-1}$; $B_{\text{max}} = 0.9 \pm 0.1$ $[^3\text{H}]$ cGMP/PDE). B, dissociation kinetics were determined at 37°C by first adding 500 nM $[^3\text{H}]$ cGMP to ~ 6 nM nPDE-S (circles) or P $\alpha\beta$ -S (squares) and incubating for 30 or 2 min, respectively. Dissociation was initiated by addition of 1 mM (final concentration) unlabeled cGMP, and samples were filtered at the indicated times thereafter. The curves represent the fit of the data to a single exponential decay function for both nPDE-S ($k_{-1} = 5.8 \pm 0.6 \times 10^{-4} \text{ s}^{-1}$; $B_{\text{max}} = 1.9 \pm 0.1$ cGMP/PDE) and P $\alpha\beta$ -S ($k_{-1} = 7.3 \pm 0.7 \times 10^{-3} \text{ s}^{-1}$; $B_{\text{max}} = 0.9 \pm 0.1$ cGMP/PDE). The symbols represent individual determinations from one experiment; see Table I for average values for n separate determinations of the rate constants.

since purified nPDE-M to which recombinant P δ has been added is able to exchange endogenous cGMP at both noncatalytic sites in the absence of membrane attachment.

Physiological Significance of Noncatalytic cGMP-binding Sites on Mammalian Rod PDE Isoforms—In the dark-adapted photoreceptor, cytoplasmic cGMP levels are in the low micromolar range, and both noncatalytic sites on nPDE-S and nPDE-M will be fully occupied. The mechanism by which transducin activates PDE to lower rapidly cytoplasmic cGMP levels during visual excitation is well understood and quantitatively accounts for the rising phase of the photoresponse (for review see Ref. 1). Thus, there is no need to invoke the noncatalytic cGMP-binding sites on bovine rod PDE to describe the regula-

tion of PDE during the initial events of photo-excitation. We consider instead possible ways the noncatalytic cGMP-binding sites may be involved in later stages of the visual transduction pathway, namely recovery from light stimulation and/or light adaptation.

A role for the noncatalytic sites to buffer free cGMP levels during the recovery phase of the flash photoresponse has been proposed for amphibian rod photoreceptors (12). In this model, the noncatalytic sites serve to buffer cytoplasmic cGMP levels in the dark, and upon PDE activation release bound cGMP to accelerate the return to the resting state. Our data show that activation of mammalian rod PDE by removing the P γ subunit results in the immediate loss of detectable binding to one of the noncatalytic sites on both PDE-M and PDE-S. This rapidly dissociating class of sites has the potential to release its bound cGMP on the same time scale as recovery phase of the photoresponse (<1 s in mammalian photoreceptors (31, 32)). However, upon cGMP release from the bound state, it is likely that the free cGMP would be destroyed by the still-active catalytic sites and therefore not contribute to elevating the cytoplasmic cGMP levels during photoresponse recovery. This conclusion is supported by recent measurements of cGMP dissociation and hydrolysis in amphibian rod outer segment suspensions (33).

An alternative hypothesis is that the noncatalytic sites on PDE may indirectly regulate the lifetime of transducin-activated PDE via modulation of P γ binding affinity to P $\alpha\beta$ (10). This idea is based on the following observations in amphibian and mammalian photoreceptors: removal of bound cGMP from the noncatalytic sites in frog ROS reduces P γ binding affinity to P $\alpha\beta$ (9) and correlates with an accelerated transducin GTPase activity (34); in bovine ROS, P γ serves as a GTPase accelerating factor (35, 36) acting in concert with the RGS9 protein (37, 38). Accordingly, cGMP dissociation from the rapidly dissociating class of sites on activated PDE might signal P γ to interact with RGS9 to stimulate GTPase activity of transducin to inactivate PDE during the recovery phase of the photoresponse.

cGMP dissociation from the second high affinity class of binding sites on bovine rod PDE is too slow ($t_{1/2} \sim 1.6$ min; Table I) to be implicated in the recovery process of the dark-adapted photoresponse. It is possible that cGMP dissociation from these noncatalytic sites may act to reduce gradually the lifetime of activated PDE during adaptation to continuous illumination and thereby lead to the smaller, faster responses characteristic of the light-adapted state. Coles and Yamane (39) and Cervetto *et al.* (40) have shown a gradual acceleration of recovery of the flash photoresponse when amphibian rod photoreceptors are exposed to continuous illumination; this response acceleration slowly develops over the same general time frame as cGMP dissociation from the higher affinity noncatalytic sites on PDE. Future work is needed to establish whether a strict temporal correlation exists between occupancy of cGMP at the noncatalytic sites and the kinetics of the recovery phase of the light-adapted photoresponse, and whether these studies performed with lower vertebrates are relevant to the regulation of mammalian rod phototransduction.

In conclusion, cGMP binding and dissociation at the noncatalytic sites on the photoreceptor PDE may indirectly regulate the enzyme by affecting the strength of the interaction of the P γ subunit with the catalytic subunits. This in turn may direct whether P γ interacts with the P $\alpha\beta$ dimer to regulate catalytic activity or with transducin and its GTPase-accelerating protein, RGS9, to regulate the kinetics of transducin inactivation. In addition, there is conflicting evidence at present (9, 41) as to whether the noncatalytic sites can allosterically regulate hydrolytic activity at the active sites, as has been demonstrated for PDE2 (6). The results in this paper provide a strong foun-

duction for unraveling the complex interplay between the non-catalytic and catalytic sites on photoreceptor PDE and the low molecular weight P γ and P δ subunits that interact with and regulate the action of this central effector enzyme in visual transduction.

Acknowledgments—We thank the reviewers for their insightful comments and assistance in preparing the revised version of the manuscript.

REFERENCES

- Pugh, E. N., Jr., and Lamb, T. D. (1993) *Biochim. Biophys. Acta* **1141**, 111–149
- Helmreich, E. J. M., and Hofmann, K. P. (1996) *Biochim. Biophys. Acta* **1286**, 285–322
- Palczewski, K., and Saari, J. C. (1997) *Curr. Opin. Neurobiol.* **7**, 500–504
- Beavo, J. A. (1995) *Physiol. Rev.* **75**, 725–748
- Burns, F., Zhao, A. Z., and Beavo, J. A. (1996) *Adv. Pharmacol.* **36**, 29–48
- Martins, T. J., Mumby, M. C., and Beavo, J. A. (1982) *J. Biol. Chem.* **257**, 1973–1979
- Yamazaki, A., Sen, I., Bitensky, M. W., Casnellie, J. E., and Greengard, P. (1980) *J. Biol. Chem.* **255**, 11619–11624
- Yamazaki, A., Bartucci, F., Ting, A., and Bitensky, M. W. (1982) *Proc. Natl. Acad. Sci. U. S. A.* **79**, 3702–3706
- Arshavsky, V. Y., Dumke, C. L., and Bownds, M. D. (1992) *J. Biol. Chem.* **267**, 24501–24507
- Cote, R. H., Bownds, M. D., and Arshavsky, V. Y. (1994) *Proc. Natl. Acad. Sci. U. S. A.* **91**, 4845–4849
- Cote, R. H., and Brunnock, M. A. (1993) *J. Biol. Chem.* **268**, 17190–17198
- Yamazaki, A., Bondarenko, V. A., Dua, S., Yamazaki, M., Usukura, J., and Hayashi, F. (1996) *J. Biol. Chem.* **271**, 32495–32498
- Baehr, W., Devlin, M. J., and Applebury, M. L. (1979) *J. Biol. Chem.* **254**, 11669–11677
- Gillespie, P. G., Prusti, R. K., Apel, E. D., and Beavo, J. A. (1989) *J. Biol. Chem.* **264**, 12187–12193
- Florio, S. K., Prusti, R. K., and Beavo, J. A. (1996) *J. Biol. Chem.* **271**, 24036–24047
- Gillespie, P. G., and Beavo, J. A. (1989) *Proc. Natl. Acad. Sci. U. S. A.* **86**, 4311–4315
- Gillespie, P. G., and Beavo, J. A. (1988) *J. Biol. Chem.* **263**, 8133–8141
- Hurwitz, R. L., Bunt-Milam, A. H., and Beavo, J. A. (1984) *J. Biol. Chem.* **259**, 8612–8618
- Miki, N., Baraban, J. M., Keirns, J. J., Boyce, J. J., and Bitensky, M. W. (1975) *J. Biol. Chem.* **250**, 6320–6327
- Hurley, J. B., and Stryer, L. (1982) *J. Biol. Chem.* **257**, 11094–11099
- Catty, P., and Deterre, P. (1991) *Eur. J. Biochem.* **199**, 263–269
- Artemyev, N. O., Natochin, M., Busman, M., Schey, K. L., and Hamm, H. E. (1996) *Proc. Natl. Acad. Sci. U. S. A.* **93**, 5407–5412
- Artemyev, N. O., Arshavsky, V. Y., and Cote, R. H. (1998) *Methods* **14**, 93–104
- Hamilton, S. E., Prusti, R. K., Bentley, J. K., Beavo, J. A., and Hurley, J. B. (1993) *FEBS Lett.* **318**, 157–161
- Cote, R. H., Nicol, G. D., Burke, S. A., and Bownds, M. D. (1989) *J. Biol. Chem.* **264**, 15384–15391
- Cote, R. H. (1999) *Methods Enzymol.* **316**, in press
- Gillespie, P. G., and Beavo, J. A. (1989) *Mol. Pharmacol.* **36**, 773–781
- Laemmli, U. K. (1970) *Nature* **227**, 680–685
- Gallagher, S. (1998) in *Current Protocols in Protein Science* (Coligan, J. E., Dunn, B. M., Ploegh, H. L., Speicher, D. W., and Wingfield, P. T., eds) pp. 10.10.1–10.10.12J. John Wiley & Sons, Inc., New York
- Bradford, M. M. (1976) *Anal. Biochem.* **72**, 248–254
- Baylor, D. A., Nunn, B. J., and Schnapf, J. L. (1984) *J. Physiol.* **357**, 575–607
- Lyubarsky, A. L., and Pugh, E. N., Jr. (1996) *J. Neurosci.* **16**, 563–571
- Calvert, P. D., Ho, T. W., LeFebvre, Y. M., and Arshavsky, V. Y. (1998) *J. Gen. Physiol.* **111**, 39–51
- Arshavsky, V. Y., and Bownds, M. D. (1992) *Nature* **357**, 416–417
- Angleon, J. K., and Wensel, T. G. (1994) *J. Biol. Chem.* **269**, 16290–16296
- Arshavsky, V. Y., Dumke, C. L., Zhu, Y., Artemyev, N. O., Skiba, N. P., Hamm, H. E., and Bownds, M. D. (1994) *J. Biol. Chem.* **269**, 19882–19887
- He, W., Cowan, C. W., and Wensel, T. G. (1998) *Neuron* **20**, 95–102
- Tsang, S. H., Burns, M. E., Calvert, P. D., Gouras, P., Baylor, D. A., Goff, S. P., and Arshavsky, V. Y. (1998) *Science* **282**, 117–121
- Coles, J. A., and Yamane, S. (1975) *J. Physiol.* **247**, 180–207
- Cervetto, L., Torre, V., Pasino, E., Marroni, P., and Capovilla, M. (1984) in *Photoreceptors* (Borsellino, A., and Cervetto, L., eds) pp. 159–175, Plenum Publishing Corp., New York
- Granovsky, A. E., Natochin, M., McEntaffer, R. L., Haik, T. L., Francis, S. H., Corbin, J. D., and Artemyev, N. O. (1998) *J. Biol. Chem.* **273**, 24485–24490